Time-resolved spectroscopic study of the excited-state spin-phonon interaction in ruby

J. E. Rives and R. S. Meltzer
Department of Physics and Astronomy, University of Georgia, Athens, Georgia 30602
(Received 21 April 1977)

The time evolution of the non-spin-flip $2\bar{A} \leftrightarrow \bar{E}$ spin-lattice relaxation in ruby has been studied with subnanosecond time resolution, following excitation of the broadband Cr^{3+} states with a N_2 laser pumped-tunable-dye laser. From the short-time dependence of the R_1 and R_2 emission we directly obtain $T_1 = 1.1$ ns for this relaxation. The branching ratio for relaxation from the broadband states to the $\bar{E}$ and $2\bar{A}$ states, respectively, is found to be 2.6. The significance of these measurements in relation to previous estimates of T_1 and to recent 29-cm^{-1} phonon spectroscopy is discussed.

I. INTRODUCTION

There have been several recent successful attempts to monoenergetically generate and/or detect high-energy acoustic phonons in ruby using the $2\bar{A} \rightleftharpoons \bar{E}$ excited-state spin-phonon interaction. Renk and Peckenzell[1] used this transition to resonantly trap 29-cm^{-1} phonons from heat pulses in order to obtain the lifetime of 29-cm^{-1} phonons in ruby. Dijkhuis *et al.*,[2] using cw optical generation and detection techniques, were able to examine the spectral width and spectral diffusion of these optically generated 29-cm^{-1} phonons. Meltzer and Rives[3] have used this resonance as a pulsed source of 29-cm^{-1} phonons to examine the time evolution of the 29-cm^{-1} phonon population and have remeasured the lifetime of these phonons.

All of the above experiments depend upon the $2\bar{A} \rightleftharpoons \bar{E}$ spin-lattice relaxation for the production and/or detection of 29-cm^{-1} phonons. It is therefore of considerable importance to examine in detail the spin-phonon interaction responsible for the phonon generation and detection processes. In this paper, we measure directly the $2\bar{A} \rightleftharpoons \bar{E}$ spin-lattice relaxation time for the non-spin-flip single-phonon processes and obtain the branching ratio for nonradiative relaxation from the broadband Cr^{3+} states to the $\bar{E}$ and $2\bar{A}$ excited states. Relaxation from the broadband states has been used in all these optical-phonon generation experiments to populate the $2\bar{A}$ state. A knowledge of the branching ratio is necessary in order to determine the efficiency for 29-cm^{-1} phonon generation.

In Sec. II we describe the experiments and our measurements. In Sec. III we consider the rate equations for the $\bar{E}$, $2\bar{A}$, and phonon populations required to analyze the time-resolved emission spectrum and consider some typical numerical solutions. In Sec. IV we determine, from a comparison of the observed data and these numerical solutions, the parameters in the rate equations. We show that the $2\bar{A} \rightleftharpoons \bar{E}$ non-spin-flip relaxation time at low temperatures is $T_1 = 1.1$ ns, more than three times larger than estimates based upon studies[4] of the Orbach contribution to the spin-lattice relaxation within $\bar{E}$, and that the branching ratio for relaxation from the broadband states favors $\bar{E}$ by a factor of 2.6 relative to $2\bar{A}$ yielding a phonon-conversion efficiency of about 28% relative to the number of absorbed photons.

II. EXPERIMENTAL

The $2\bar{A} \rightleftharpoons \bar{E}$ spin-phonon interaction is examined from the time evolution of the R_2 and R_1 emission after pulsed excitation into the broadband absorption (see Fig. 1) with a N_2 laser-pumped pulsed tunable dye laser. About 20 μJ of energy at ~5800 Å are focused to a rectangle ~0.2 × 3 mm on a 1 mm thick slab of 0.06% ruby, producing a nearly uniform excitation density along the laser beam. After excitation, the broadband states rapidly

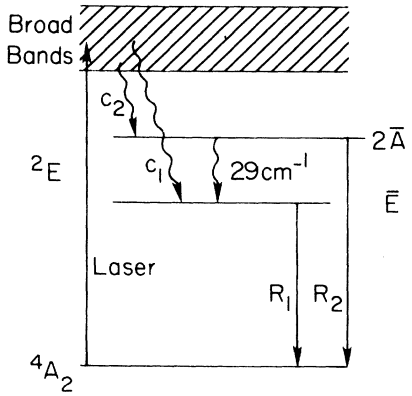

FIG. 1. Energy-level diagram of Cr^{3+} in Al_2O_3 showing the pumping scheme and relaxation mechanisms. The broadband states, after pumping with a pulsed tunable dye laser, relax to $\bar{E}$ and $2\bar{A}$ with a branching ratio c_1/c_2. Those ions decaying through $2\bar{A}$ generate 29-cm^{-1} phonons. The population of $2\bar{A}$ and $\bar{E}$ is monitored from the R_2 and R_1 emission.

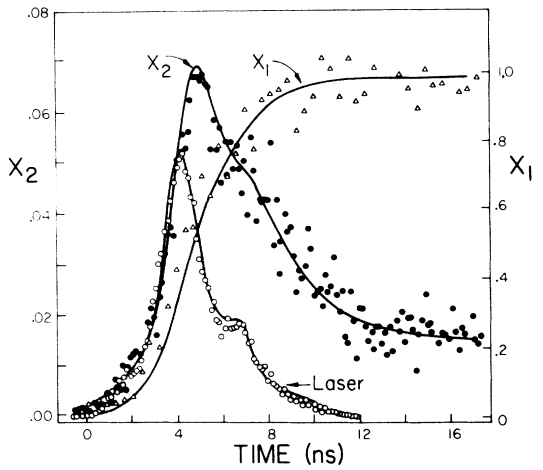

FIG. 2. Normalized emission from $2\bar{A}(x_2)$ and $\bar{E}(x_1)$ after pumping the broadband states. The open circles show the laser pulse; the closed circles and triangles indicate the normalized R_2 and R_1 emission, respectively. The solid curves show the best numerical solutions to the rate equations with $T_1 = 1.1$ ns, branching ratio $= 2.6$, $T_{ph} = 37.5$ ns, and $b = 0.08$.

relax ($T_{band} \ll 1$ ns) to the $2\bar{A}$ and $\bar{E}$ states. At low temperatures, those ions which decay via the $2\bar{A}$ states further relax to $\bar{E}$ by means of 29-cm^{-1} single-phonon emission. During the relaxation processes, the $2\bar{A}$ population is above its thermal equilibrium value while the ^2E states thermalize. In addition, the 29-cm^{-1} phonons can be resonantly absorbed and reemitted by the excited Cr^{3+} ions, causing diffusive phonon motion and a phonon bottleneck, whereby the $2\bar{A}$ population can remain enhanced for a time $\tau \gg T_1$ until the phonons either diffuse out of the excited region, or undergo inelastic scattering, removing them from the resonant channel. It is the early dependence of the R_2 emission, before development of the phonon bottleneck,[5] that provides the information concerning the spin-phonon interaction of interest in this paper.

The time evolution of the R_2 and R_1 emission is obtained with subnanosecond time resolution using the single-photon time correlation technique. Since this has been described in some detail elsewhere,[6] we discuss it only briefly here. The time difference between the laser excitation pulse (start pulse) and the detection of a single emitted photon (stop pulse) is obtained from a time-to-amplitude convertor, the output of which is stored on a pulse height analyzer. This operation is performed ~10^6 times producing a histogram of the time distribution of emitted photons.

A typical histogram of the laser pulse, R_1 and R_2 emission is shown in Fig. 2. The laser-pulse data were obtained by selecting for the stop-pulse detected photons from the back reflection of the laser off the front surface of the crystal. The laser pulse is asymmetric with a 2 ns full width at half-maximum. The R_2 emission shows first a rapid buildup as the broadband relaxation pumps the $2\bar{A}$ state and then a rapid decay as the ^2E states relax with 29-cm^{-1} phonon generation. The R_2 emission remains enhanced, however, as the phonon bottleneck develops. The decay time of the bottleneck and the level at which the bottleneck develops depends on the laser energy as shown previously.[3]

III. RATE EQUATIONS

The two-level spin-lattice relaxation between the $2\bar{A}$ and $\bar{E}$ states in ruby can be described by standard rate equations,[7] modified to explicitly include the laser pumping function. If n_1 and n_2 are the populations of the $\bar{E}$ and $2\bar{A}$ states, respectively, the total excited-state population N^* is $n_1 + n_2$. In terms of the normalized populations, $x_1 = n_1/N^*$ and $x_2 = n_2/N^*$, the rate equations are

$$\frac{dx_1}{dt} = -T_1^{-1}[x_1\bar{p} - x_2(\bar{p}+1)] + \frac{c_1F(t)}{N^*},$$

$$\frac{dx_2}{dt} = T_1^{-1}[x_1\bar{p} - x_2(\bar{p}+1)] + \frac{c_2F(t)}{N^*}, \qquad (1)$$

$$\frac{dp}{dt} - T_{ph}^{-1}\bar{p} - bT_1^{-1}[x_1\bar{p} - x_2(\bar{p}+1)],$$

where $\bar{p}$ is the average resonant-phonon occupation number,[8] T_1 is the spin-lattice relaxation time, T_{ph} is the resonant-phonon lifetime, and $b = N^*/\Sigma$ is the bottleneck factor with $\Sigma = 12\pi\nu^2\Delta\nu/v^3$, the number of phonon modes within the resonant width $\Delta\nu$. It has been assumed in Eqs. (1) that $T_{band} \ll T_1$, so that $F(t)$ just represents the time dependence of the laser output, and c_1/c_2 is the branching ratio from the broadband to the $\bar{E}$ and $2\bar{A}$ Cr^{3+} states, respectively. The total excited-state population N^* is $\int F(t)\,dt$. If the laser function $F(t)$ is known, the rate equations can be solved numerically for the time dependence of x_1, x_2, and $\bar{p}$.

Typical numerical solutions for the time dependence of x_2 are shown in Fig. 3 for a range of values of the bottleneck factor b. The laser pulse shown in Fig. 2 was used for these calculations, and values for T_1 and T_{ph} of 1.0 and 40.0 ns, respectively, were chosen to be close to the best fit values for this experiment as discussed in Sec. IV.

Initially x_2 increases rapidly in response to the laser pumping. For $b < 1.0$ the slower bottlenecked decay, at the rate $\tau^{-1} = T_{ph}^{-1}(1+b)$, develops only after a sufficient phonon population is built up by the spin-lattice relaxation at the rate T_1^{-1}. The height of the resulting peak in x_2 in these cases

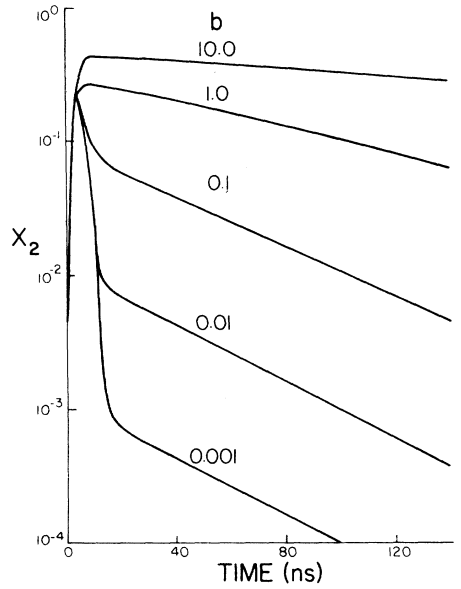

FIG. 3. Time dependence of the numerical solutions to the rate equation for x_2, the normalized R_2 emission, as a function of b. In these calculations, $T_1 = 1.0$ ns, branching ratio = 1, and $T_{ph} = 40$ ns. Note the development of the phonon bottleneck at about 20 ns.

is determined primarily by the branching ratio c_1/c_2 and T_1, while the separation in time between the laser peak and the peak in x_2 depends mainly on T_1.

An analysis of the short-time behavior of the measured values of x_1 and x_2, therefore, provides a direct determination of the spin-lattice relaxation time T_1 and the branching ratio. Analysis of the bottlenecked decay yields the value of the bottleneck factor b and the phonon lifetime T_{ph} for the particular experimental conditions.

IV. RESULTS AND DISCUSSION

The time evolution of the normalized $\bar{E}(x_1)$ and $2\bar{A}(x_2)$ populations,[9] shown in Fig. 2, was compared with numerical solutions to the rate equation in order to extract values for the parameters T_1, c_1/c_2, b, and T_{ph}. In order to obtain a reliable fit to the data it was necessary to express the laser function $F(t)$ in analytic form for input into the computer program. An asymmetric Lorentzian of the form $f(t) = At/[\Delta t^2 + (t - t_0)^2]$ with an appropriate cutoff was found to provide a good fit for the pulse, except for the small shoulder at about $t = 6$ ns. Adding a small Gaussian contribution around $t = 6$ ns produced an excellent fit of the entire pulse. A good estimate of T_{ph} was obtained directly from the $R_2(x_2)$ data in the bottlenecked regime. The four parameters were then varied to produce the best fit to the R_1 and R_2 data, shown as solid curves through the data in Fig. 2. Also shown is the analytic fit to the laser pulse. The best values for T_1 and c_1/c_2 are

$$T_1 = 1.1 \pm 0.3 \text{ ns},$$

and the branching ratio is

$$c_1/c_2 = 2.6 \pm 0.2.$$

The values of b and T_{ph} will depend on the laser energy and the size of the excitation region.[3] In the present case, as discussed in Sec. II, we find

$$b = 0.08 \pm 0.01$$

and

$$T_{ph} = 37.5 \pm 2.0 \text{ ns}.$$

These values are consistent with those found in earlier measurements on this same crystal.[3]

The data also indicate that $T_{band} < 0.3$ ns. This justifies our assumption that $T_{band} \ll T_1 = 1.1$ ns, from which we concluded that $\bar{E}$ and $2\bar{A}$ are pumped with a time dependence identical to that of the laser-excitation source.

The above value of $T_1 = 1.1$ ns is about 40% of the value obtained by Kurnit *et al.*[10] in a photon-echo experiment. The difference may be due to the presence of a phonon bottleneck in the photon-echo experiment. In that case, the high concentration of excited Cr^{3+} ions produced with the ruby laser may have depleted the resonant-phonon population leading to an increase in the observed relaxation time.[11] On the other hand, our value of T_1 is about 3–4 times larger than that obtained in indirect measurements by Geschwind *et al.*[4] and by Lengfeller *et al.*[12] Geschwind based their value on a measurement of the Orbach contribution to the spin-lattice relaxation rate within the $^2E(\bar{E})$ state. They obtained a value of 16 ns for the spin-flip relaxation time between $2\bar{A}$ and $\bar{E}$ which when coupled with a calculation of 50 for the ratio of the non-spin-flip to spin-flip relaxation rates by Blume *et al.*[13] implies 0.3 ns for the non-spin-flip relaxation time. Our direct measurement of T_1 taken with Geschwind's results implies a value of 15 for this ratio. Lengfeller observed the $\bar{E} \rightarrow 2\bar{A}$ resonance width in an excited-state infrared-absorption experiment. The line was nearly Lorentzian with a 360-MHz width. Assuming that this width is limited solely by the $2\bar{A} \rightarrow \bar{E}$ relaxation they obtained a value of $T_1 = 0.44$ ns. However, there may be a significant contribution from inhomogeneous broadening implying a somewhat longer relaxation time.

Finally we note that the value of 2.6 for the branching ratio implies a 28% efficiency for conversion of absorbed photons to 29-cm^{-1} acoustic phonons.

ACKNOWLEDGMENT

We thank Dr. William Yen for loaning us the ruby sample.

[1]K. F. Renk and J. Peckenzell, J. Phys. (Paris) Colloq. 33, C4-103 (1972). See also, K. F. Renk and J. Deisenhofer, Phys. Rev. Lett. 26, 764 (1971).

[2]J. I. Dijkhuis, A. van der Pol, and H. W. deWijn, Phys. Rev. Lett. 37, 1554 (1976).

[3]R. S. Meltzer and J. E. Rives, Phys. Rev. Lett. 38, 421 (1977).

[4]S. Geschwind, G. E. Devlin, R. L. Cohen, and S. R. Chinn, Phys. Rev. 137, A1087 (1965).

[5]Although the resonant phonon temperature builds up in a time $\approx T_1$, these phonons do not enhance the $2\bar{A}$ population until they are resonantly absorbed. In the present experiments with $b \approx 0.08$ the phonon time of flight before absorption is about 14 ns. We therefore speak of times earlier than 14 ns as being before the development of the phonon bottleneck.

[6]R. S. Meltzer and R. M. Wood, Appl. Optics 16, 1432 (1977).

[7]See, for instance, A. Abragam and B. Bleaney, *Electron Paramagnetic Resonance of Transition Ions* (Clarendon, Oxford, 1970), Chap. 10.

[8]The thermal-equilibrium average-phonon occupation number at the bath temperature T_0 is $\bar{p}_0 = [\exp(h\nu/kT_0) - 1]^{-1}$. In the present case $\bar{p} > \bar{p}_0$ so long as x_2 exceeds its thermal equilibrium value.

[9]The relative-emission intensities were corrected for the relative-emission strengths to obtain the populations.

[10]M. A. Kurnit, I. D. Abella, and S. R. Hartmann, in *The Physics of Quantum Electronics Conference Proceedings, San Juan, Puerto Rico, 1965*, edited by P. L. Kelley, B. Lax, and P. E. Tannenwald (McGraw-Hill, New York, 1966), p. 267.

[11]R. S. Meltzer and J. E. Rives, Phys. Rev. B 15, 2442 (1977).

[12]H. Lengfeller, G. Pauli, W. Heisel, and K. F. Renk, Appl. Phys. Lett. 29, 566 (1976).

[13]M. Blume, R. Orbach, A. Kiel, and S. Geschwind, Phys. Rev. 139, A314 (1965).